Preparation and surface morphology of black lithium tantalate wafers

XUEFENG XIAO[1,2,3*,+], QINGYAN XU[1,2,3,+], HUAN ZHANG[1,2], LINGLING MA[1,2], LIAN HAI[1,2], XUEFENG ZHANG[3]
[1]*College of Electric and Information Engineering, North Minzu University, Yinchuan, 750021, China*
[2]*Key Laboratory of Physics and Photoelectric Information Functional Materials Sciences and Technology, North Minzu University, Yinchuan, 750021, China*
[3]*Ningxia Ju Jing Yuan Crystal Technology Company Limited, Shizuishan 753000, China*
[+]*Both authors contributed equally to this work*

Black lithium tantalate (BLT) wafers were prepared by annealing and reduction; a mixture of high purity aluminium powder and silicon powder were used as a reducing agent. The congruent lithium tantalate (CLT) wafers and the BLT wafers were prepared by reduction under different conditions and taken as the research objects. The surface of CLT wafers after annealing and reduction showed uniform orange-peel morphology by scanning electron microscope observation; the surface oxygen content was reduced and uniform. However, a local dark orange-peel spot formed in the wafers directly after the reduction process without annealing, and the oxygen content on the surface was reduced and uneven. Atomic force microscope observation revealed that the average surface roughness of the wafers was reduced and more uniform after annealing and reduction. The data showed that high-temperature annealing before reduction is helpful for the stress release of CLT wafers and a blackening effect is more easily achieved. The reduction treatment condition of CLT wafers determines the quality of BLT wafers. Good reduction and early treatment technology make it easy to prepare uniform and consistent blackening wafers, which can reduce the pyroelectric property of wafers and improve the yield in the subsequent process of making surface acoustic wave filter devices.

(Received February 14, 2022; accepted August 10, 2022)

Keywords: Lithium tantalate, Reduction, Scanning electron microscope (SEM), Atomic force microscope (AFM)

1. Introduction

The lithium tantalate ($LiTaO_3$, LT) crystal is generally congruent lithium tantalate crystal (CLT); CLT crystal is usually prepared by the Czochralski method, in the air or under hypoxia and the crystal is usually colourless or light yellow. The large piezoelectric coefficient of lithium tantalate crystal makes it an important substrate material for low insertion loss on surface acoustic wave (SAW) filters. However, the pyroelectric effect of materials brings unavoidable difficulties to the fabrication and application of devices. LT crystals have a high pyroelectric coefficient, and the surface of the wafer is prone to a large amount of surface electrostatic charge accumulation due to temperature changes, which can be released spontaneously between fork electrodes, between wafers and between the wafer and the fixture. When the electrostatic field reaches a certain degree, wafer cracking, microdomain inversion and fork electrode burning will occur, which greatly reduces the yield of the device. The pyroelectric effect of LT wafers after reduction treatment is significantly reduced and the generation of electrostatic field can be avoided [1-12].

Researchers generally use H_2, toner or a mixture of iron and lithium carbonate as a reducing agent to prepare BLT wafers, known as black wafers, to eliminate the thermoelectric effects and reduce transmittance [5,6,13,14]. In this paper, the BLT wafers were prepared by mixed reduction of aluminium powder and silicon powder. Scanning electron microscope (SEM) and atomic force microscope (AFM) were used to investigate the oxygen, tantalum ratio and surface morphology of BLT and CLT wafers.

2. Experimental

2.1. Reduction of lithium tantalate wafers

The congruent LT crystal was used in the experiment grown by the Czochralski method and crystal orientation for Y42^o direction single circular wafer polishing; the wafer size was 4 inches with a thickness of 0.25 mm. CLT wafers were divided into three groups. The first group was white wafers, that is, wafers without blackening treatment. The second group did not do annealing treatment. The third group was annealed at 580 ^{o}C and treated in a reduction furnace with a mixture of aluminium powder (99%) and silicon powder (99.9999%) under the same conditions as the second group. The sponge silicon was made by crushing and grinding. The aluminium powder and silicon powder with weight ratio is 5:1 were put into the V-type mixer for 4 hours The second and third groups of wafer samples were placed into corundum tubes and the mixture of aluminium powder and silicon powder was used to bury them fully. Then, it was put into the reduction furnace and a vacuum pump was used to produce a

pressure of 0.01pa. The temperature was gradually raised to 450 ^{o}C at a rate of 50 ^{o}C/h. The temperature was maintained for 40 hours and then reduced to room temperature. The second, third and first untreated wafers were then cleaned and air-dried for analysis. Samples of 1#, 2# and 3# were CLT wafers with a size of 8×8×0.25 mm^3 after processing of the first, second and third groups, respectively. Among them, 1# was white and 3# was black. Samples 2# and 3# could not be visually distinguished [15].

2.2. Scanning electron microscopy (SEM) analysis

The SEM test was conducted with a German Zeiss company SUPRATM55 type high-resolution field emission scanning electron microscope (5kV, 30 microns standard aperture, in-lens inside the tube and secondary electron detector imaging). The Oxford-AztecX-Max80 X-ray spectrometer was used for the crystal surface micro area element analyses (18 kV, 60 microns standard aperture and high current mode). The sample was sprayed with gold before testing.

2.3. Atomic force microscope (AFM) analysis

The AFM was used for testing by Dimension Edge type atomic force microscope produced by BRUKER, Germany. The tapping mode was used for testing in the air, and the silicon probe with tip curvature radius of 8 nm and resonance frequency of 331.179 kHz was used for scanning ranges of 10×10 μm^2, 5×5 μm^2, 1×1 μm^2 and a scanning frequency of 0.5 Hz.

3. Results and discussions

3.1. Morphology of orange-peel in BLT wafers

Figs. 1, 2 and 3 show the morphologies of 1#CLT, 2#BLT and 3#BLT, respectively, under SEM. According to Fig. 1 (a), (b) and (c), there are nanometre-sized small bumps on the surface of CLT wafers; Fig. 1 (d) shows that CLT wafer is relatively flat in the micrometre-scale range. This indicated that the polished CLT wafer had a rough surface at the nanometre scale range before any treatment, which may be because the stress inside the wafer was not uniform, that is, atomic groups with different stresses were formed. Figs. 2 (a), (b), (c) and (d) show that the BLT wafers formed after direct reduction without annealing had an outer appearance of orange peel, but part of the local morphology of orange peel had a dark colour, that is, a dark orange peel spot. This is because different stress groups formed during the process of reduction due to greater local stress resulting in oxygen loss difficulties. According to Figs. 3 (a) and (b), after annealing treatment under certain conditions and reduction treatment, BLT wafers formed uniform and consistent orange peel morphology within the nanometre scale range, indicating that the reduction treatment was relatively uniform. According to a comparison between Figs. 3 (c) and (d) and Figs. 2 (e) and (f), the surface of BLT crystal that formed after annealing and reduction was flatter in the micrometre scale range. In conclusion, the reduction processing conditions of CLT wafers determines the quality of the prepared BLT wafers; good reduction and early treatment processes make easy-to-prepare uniform and consistent black wafers.

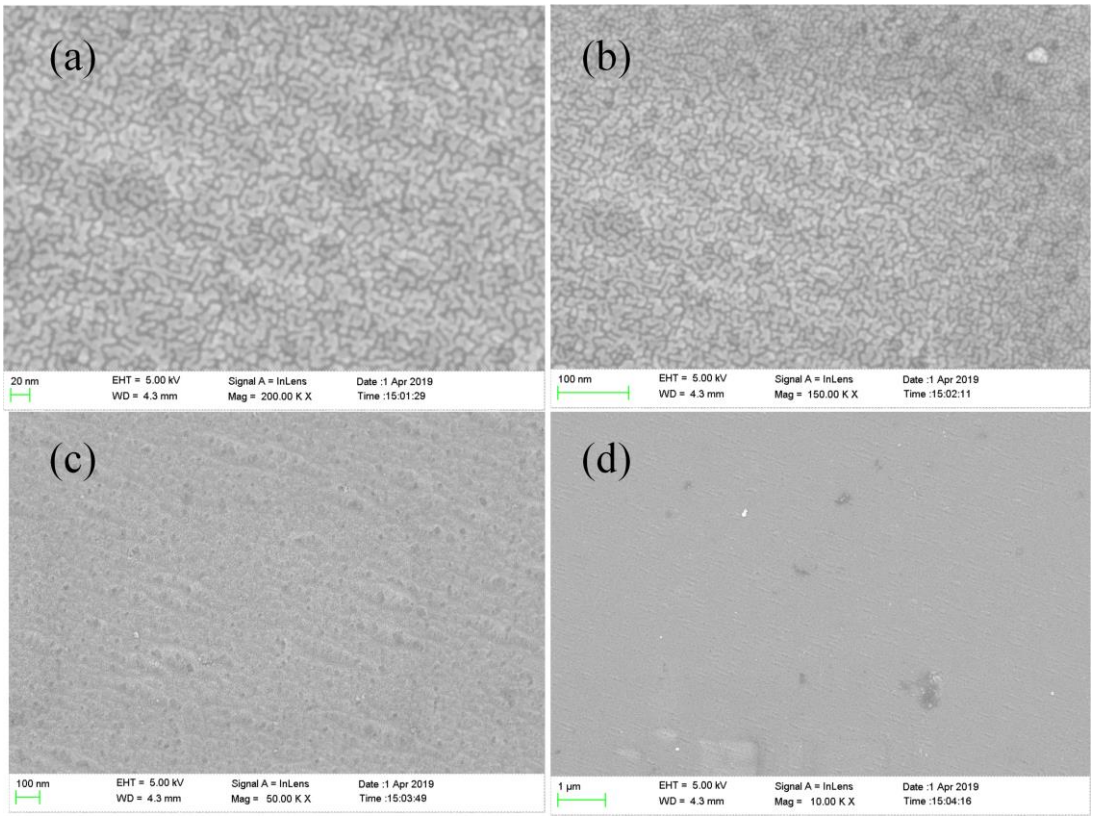

Fig. 1. SEM morphology of 1#CLT wafer

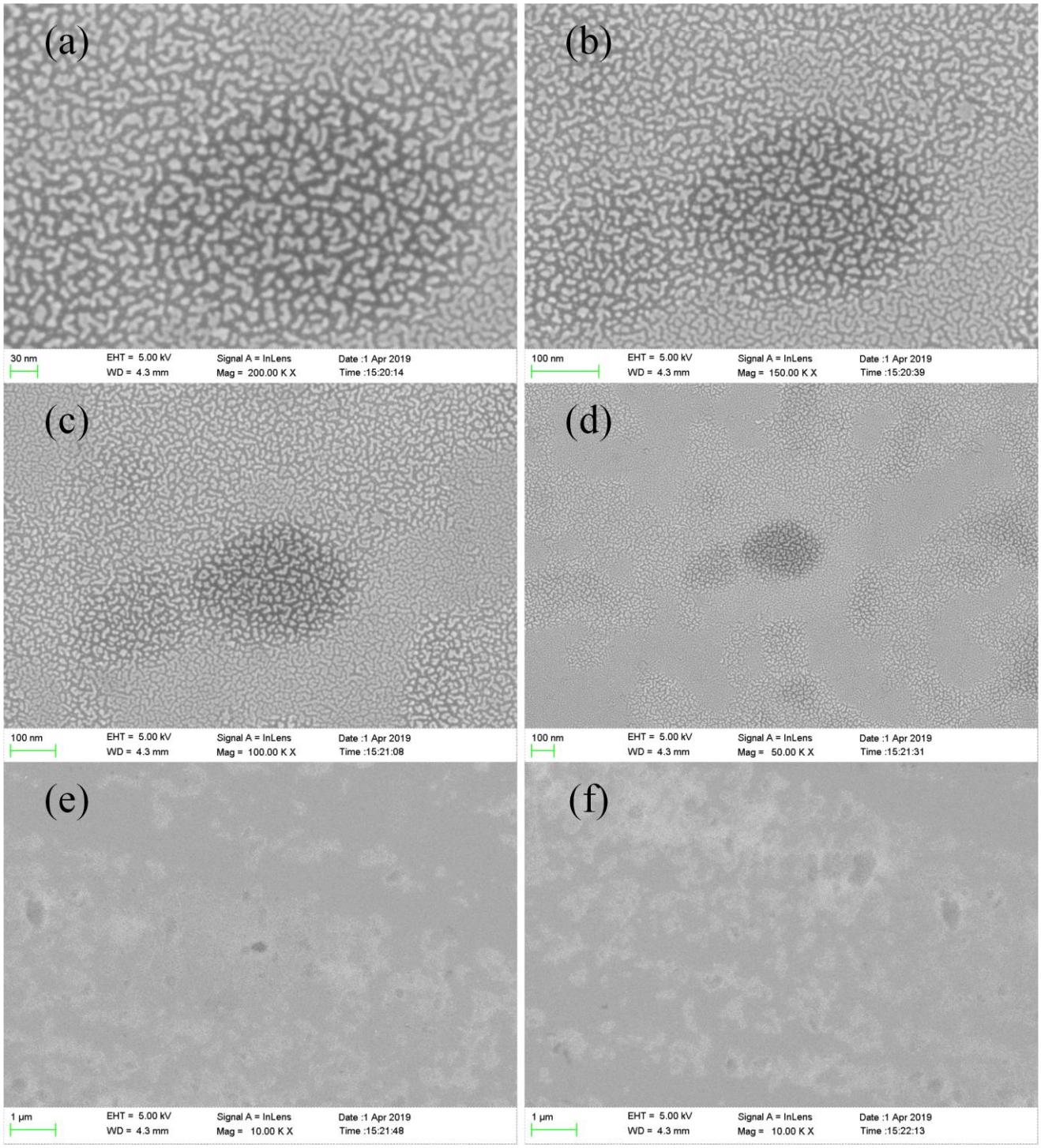

Fig. 2 . SEM morphology of dark orange peel spot of 2#BLT wafer

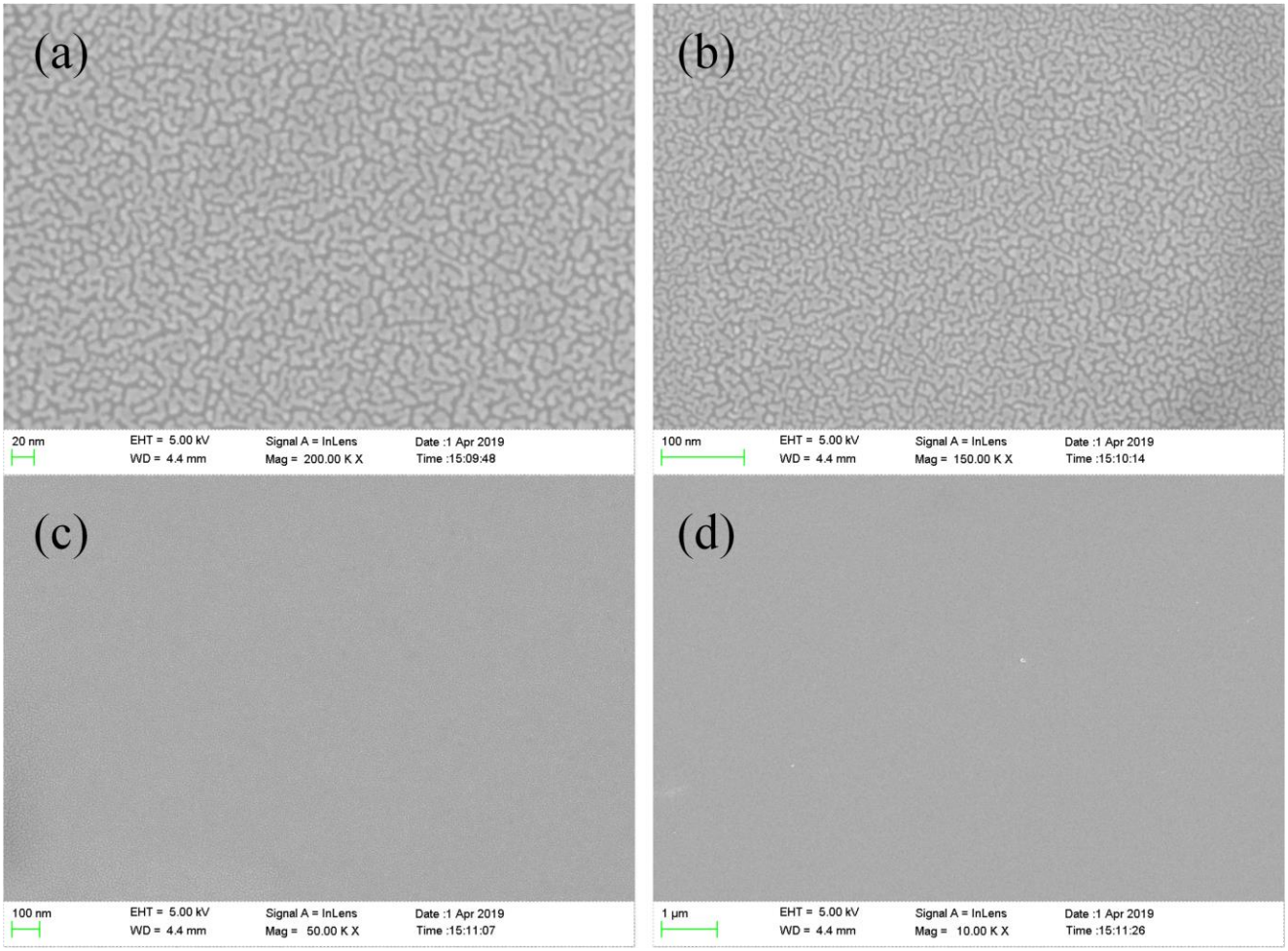

Fig. 3 . SEM morphology of uniform orange peel of 3#BLT wafer

3.2. Oxygen element content in BLT wafers

X-ray energy spectrometer was used to analyse the micro-zone elements on the crystal surface. Fig. 4 shows the qualitative analysis spectral lines of 1#CLT, 2#BLT and 3#BLT wafer samples. As can be seen from Fig. 4, all the three samples contained oxygen and tantalum, and there were no impurity elements except for lithium, indicating that the crystal growth quality was high and no other elements were mixed. Table 1 shows the quantitative percentage of the weight and the atomic number of oxygen and tantalum, corresponding to the qualitative analysis in Fig. 4; after the CLT wafer is restored, the oxygen content on the surface of the BLT wafer was reduced to different degrees, indicating that aluminium powder captures a portion of the oxygen during reduction. Table 2 shows the comparison of oxygen atomic percentage in the elemental analysis of the three samples at five points; the average oxygen element percentage in 3# BLT wafer was the lowest (76.22%) and 1# CLT wafer was the highest (76.67%). Fig. 5 shows the curve of oxygen element atomic number percentage content on the surface of the three wafers; the oxygen element atomic number percentage curve on the surface of 3#BLT wafer is close to a straight line, indicating that the oxygen element content on the surface was almost unchanged. The curve of the oxygen element atomic number percentage on the surface of the CLT polished wafer without any treatment is a broken line, which indicates that the oxygen element content on the surface of CLT polished chip changed greatly. The oxygen content on the surface of 2#BLT wafer with direct reduction without annealing was between the other samples. Fig. 6 shows the distribution of oxygen and tantalum on the surface of the three wafers; the oxygen element distribution on the 3#BLT wafer was more uniform than on the 1#CLT or 2#BLT wafer, while the tantalum element distribution is similar in each, which indicates that the mixture of aluminium powder and silicon powder as the reducing agent did not change the tantalum element distribution on the surface of the CLT wafer. In conclusion, good reduction and preliminary treatment technology can make the content of elements on the surface of the CLT wafer more uniform, uniformly rearrange the elements inside the wafer under the action of external factors.

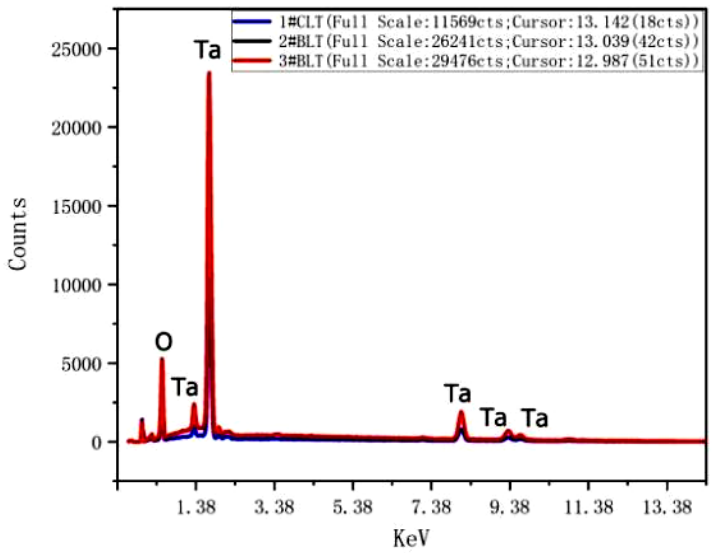

Fig. 4 . SEM-EDS energy spectra of three LT wafer samples

Table 1. Comparison of oxygen and tantalum content in three LT wafers tested by energy spectrum

Element	1#CLT		2#BLT		3#BLT	
	Weight%	Atomic%	Weight%	Atomic%	Weight%	Atomic%
O K	23.58	77.72	21.91	76.04	22.15	76.30
Ta M	76.42	22.28	78.09	23.96	77.85	23.70
Total content	100.00					

Table 2. Comparison of oxygen atom content in three LT wafers tested by energy spectrum

Sample	O K (Atomic%)					Average value
	1	2	3	4	5	
1#CLT	77.72	78.26	74.51	76.59	76.27	76.67
2#BLT	77.44	75.99	76.04	76.05	76.00	76.30
3#BLT	76.30	76.21	76.13	76.23	76.24	76.22

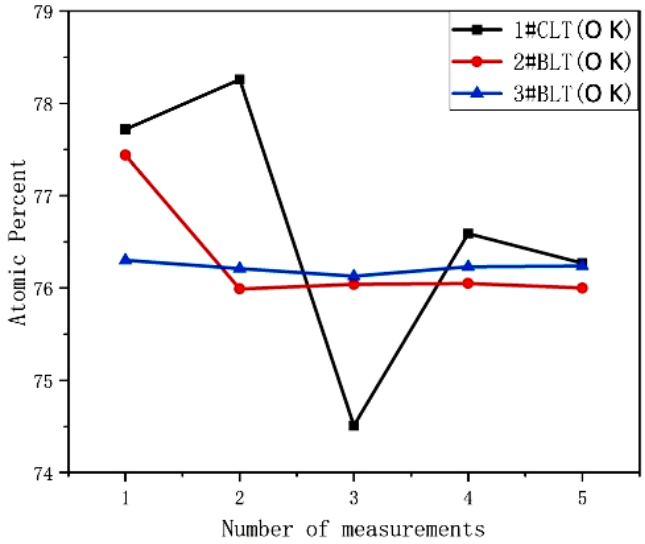

Fig. 5. Atomic number percentage of oxygen elements on the surface of the three wafers (color online)

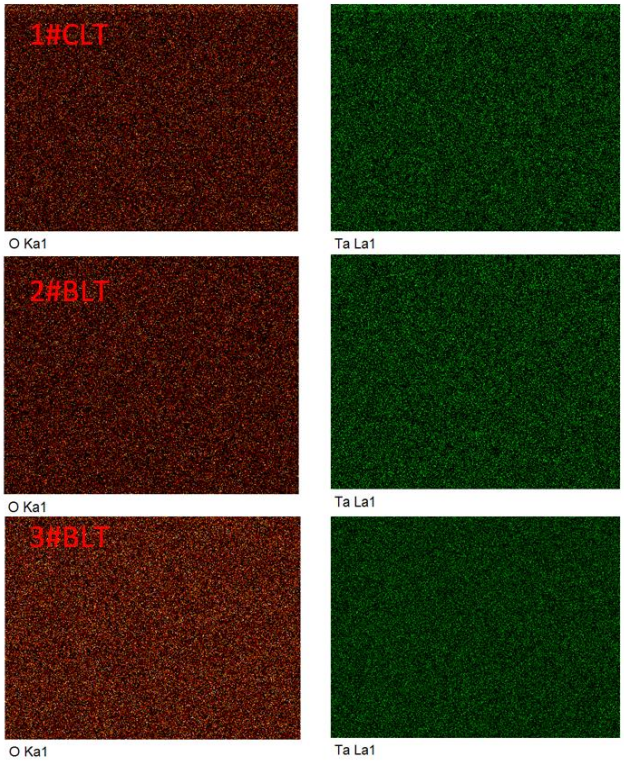

Fig. 6. Distribution of oxygen and tantalum on the surface f the three wafers (color online)

3.3. Surface morphology and roughness of BLT wafers

Figs. 7, 8 and 9 show the 2 and 3D AFM morphology of 1#CLT, 2#BLT and 3#BLT wafer surfaces, respectively. Fig. 7 shows the sags and crests of the CLT wafer surface; these were improved after direct reduction treatment (Fig. 8). The bright spots in Fig. 8 correspond to the dark orange-peel spot observed via SEM. Fig. 9 shows that the surface of the wafer became smoother after annealing and reduction treatment, this is especially visible in the two-dimensional image. According to the colours in the three pictures, Fig. 9 is lighter, while Figs. 7 and 8 are darker, indicating that the surface hardness of the wafers became soft after annealing and reduction treatment. These results support previous studies; the Vickers hardness of the three kinds of wafers have been reported to be 831.1, 806.1 and 782.7 MPa, respectively [12]. Table 3 shows the surface roughness of the three kinds of wafers, in which Rq and Ra are root mean square roughness and average roughness, respectively. Fig. 10 is the comparison chart of the surface average roughness of the three wafer samples; the surface average roughness of the 3#BLT wafer was small and almost a straight line, indicating that the surface of the CLT wafer after annealing and reduction treatment was more uniform.

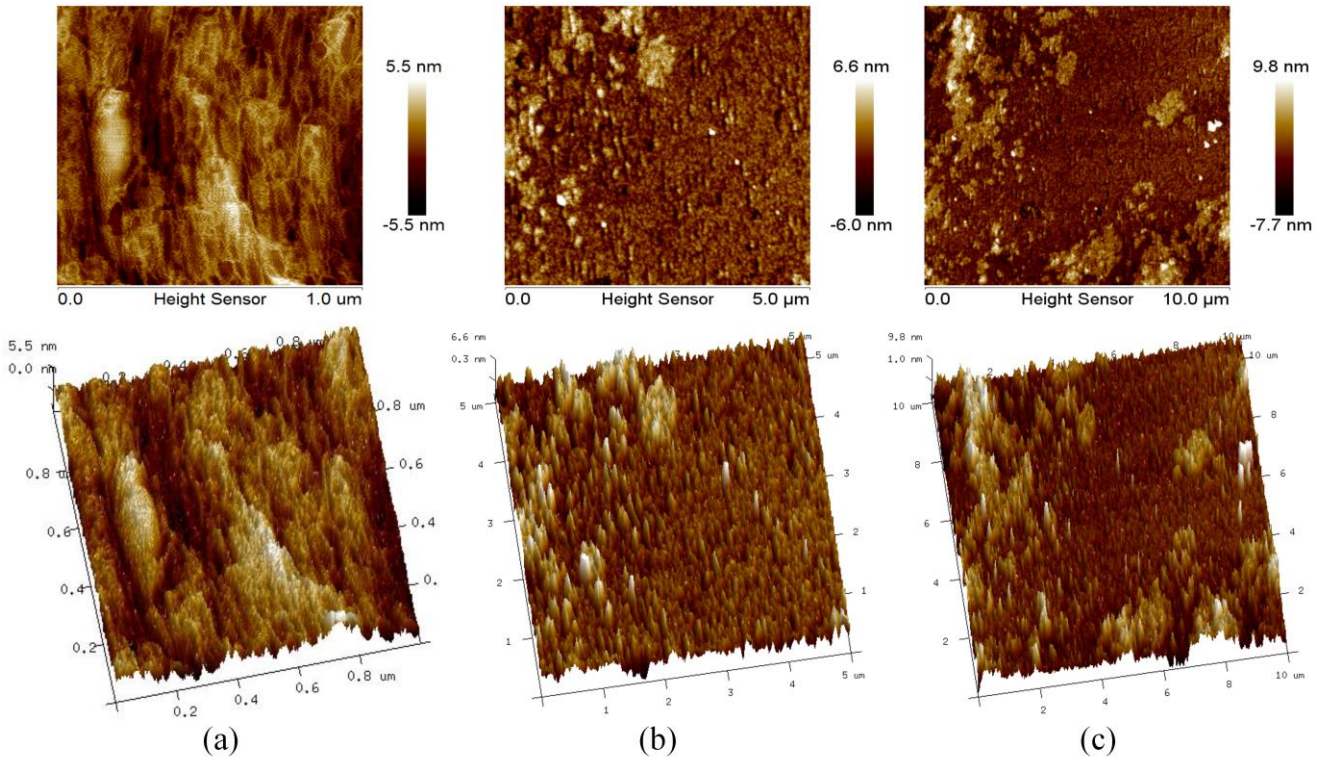

Fig. 7 . AFM images of 1#CLT wafer (color online)

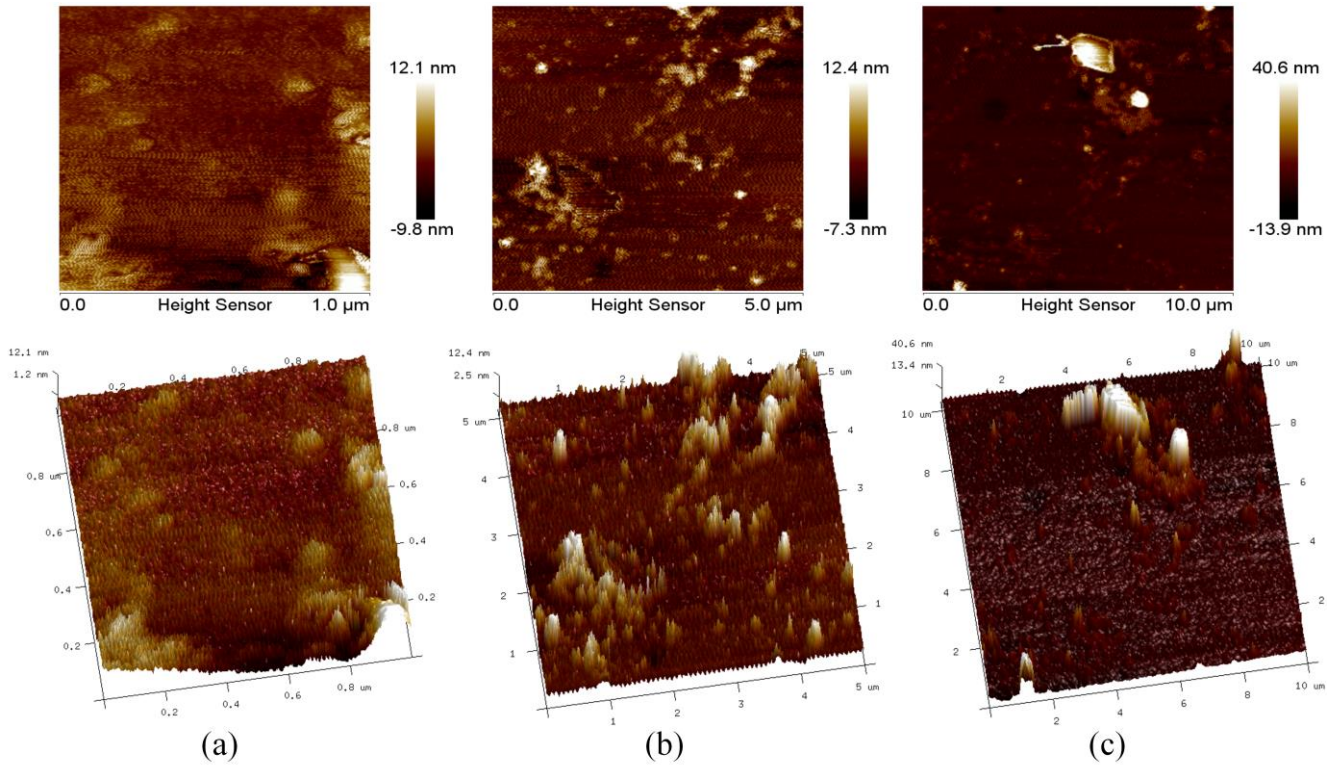

Fig. 8. AFM images of 2#BLT wafer (color online)

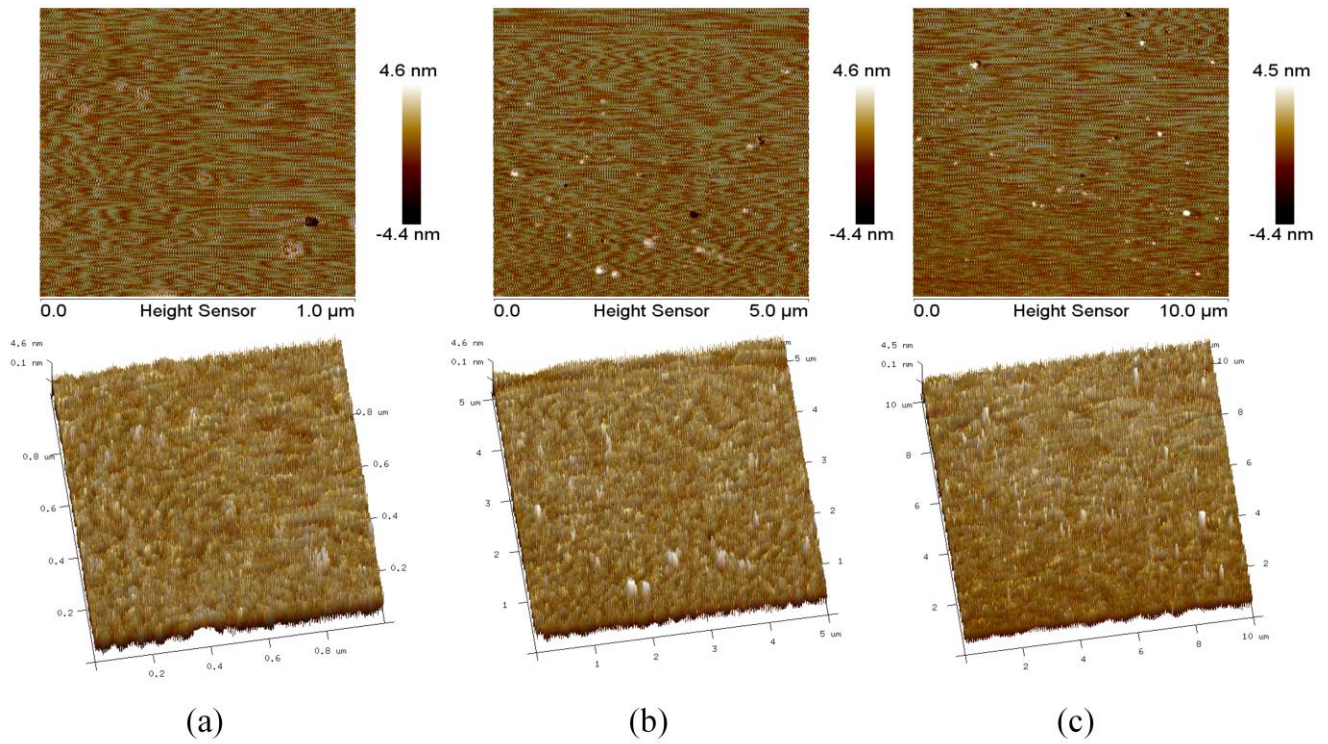

Fig. 9. AFM images of 3#BLT wafer (color online)

Table 3. Surface roughness comparison of three wafer samples

Samples	1#CLT			2#BLT			3#BLT		
Image Surface Area (μm^2)	1	25	100	1	25	100	1	25	100
Image Rq (μm)	0.00158	0.00164	0.00241	0.00254	0.00247	0.00561	0.00187	0.00186	0.00175
Image Ra (μm)	0.00127	0.00123	0.00175	0.00174	0.00173	0.00269	0.00167	0.00166	0.00154

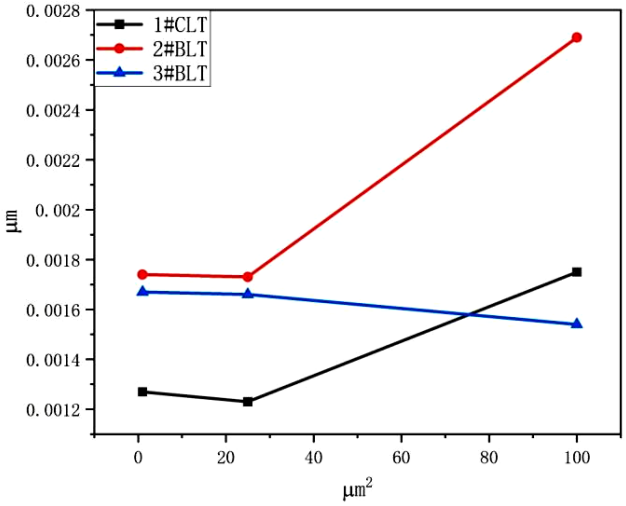

Fig. 10. Surface average roughness of three wafer samples (color online)

4. Conclusions

The mixture of aluminium powder and silicon powder as reducing agent failed to change the tantalum distribution on the surface of the CLT wafer; however, the percentage of oxygen atoms decreased and the distribution was more uniform, which indicates that some oxygen was captured by the aluminium powder on the surface of wafers during the reduction process. SEM was used to observe that the surface of lithium tantalate wafers after annealing and reduction showed uniform orange-peel morphology, and the oxygen content on the surface was reduced and uniform. The local dark orange-peel spot formed on the non-annealed wafers after a direct reduction process, and the oxygen content on the surface was reduced and uneven. The results of AFM showed that the surface average roughness of the wafer was reduced and more uniform after annealing and reduction. All of these results indicated that a good reduction and early treatment process could make the stress inside the wafer more uniform, make the element content on the surface of the CLT wafer more uniform, make the elements inside the wafer rearrange uniformly under the action of external factors and facilitate the conductivity uniformity in SAW filter devices. The reduction processing conditions of CLT wafers determine the quality of BLT wafers. Good reduction and pre-treatment technology facilitate easy-to-prepare, uniform and consistent blackening wafers. The wafers produced by reduction can effectively reduce the pyroelectric property of LT wafer and improve the yield of the SAW filter device during the subsequent manufacturing process.

Acknowledgments

This research was funded by the Fundamental Research Funds for the Central Universities, North Minzu University (2020DXXY002 and 2021KJCX07), the National Natural Science Foundation of China (61965001 and 11864001), the Ningxia Province Key Research and Development Program (2018BEE03015 and 2021BEE03005), the Natural Science Foundation of Ningxia (2019AAC03103 and 2020AAC03239), the Ningxia first-class discipline and scientific research projects (electronic science and technology) (NXYLXK2017A07). The authors thank the Ningxia new solid electronic materials and Devices research and development innovation team, the Ningxia advanced intelligent perception control innovation team and the Ningxia acoustooptic-crystals industrialization Innovation team.

References

[1] Y. Ma, X. Huang, Y. Song, W. Hang, T. Zhang, Materials **12**, 1683 (2019).
[2] W. Hang, X. Huang, M. Liu, Y. Ma, Materials **12**, 4213 (2019).
[3] Y. Ma, X. W. Huang, Y. X. Song, W. Hang, J. L. Yuan, T. H. Zhang, Materials **12**, 2799 (2019).
[4] X. Gong, M. Fang, G. Fei, M. Liu, F. Li, G. Shang, L. Zhang, RSC Adv. **5**, 31615 (2015).
[5] T. Yn, F. Zheng, Y. Yu, S. Qin, H. Liu, J. Wang, D. Yu, J. Appl. Cryst. **44**, 158 (2011).
[6] T. Ya, H. Liu, J. Wang, F. Zheng, S. Yao, Z. Xia, J. Wu, R. I. Boughton, J. Alloy. Compd. **497**, 412 (2010).
[7] J. Wu, Z. Chen, R. K. Choubey, C. Lan, Mater. Chem. Phys. **133**, 813 (2012).
[8] T. Yan, N. Ye, L. Xu, Y. Sang, Y. Chen, W. Song, X. Long, J. Wang, H. Liu, J. Phys. D: Appl. Phys. **49**, 195005 (2016).

[9] A. V. Yatsenko, M. N. Palatnikov, N. V. Sidorov, A. S. Pritulenko, S. V. Evdokimov, Phys. Solid State **57**, 1547 (2015).
[10] M. Kovar, L. Dvorak, S. Cerny, Appl. Surf. Sci. **74**, 51 (1994).
[11] D. L. Zhang, Q. Zhang, W. H. Wong, E. Y. Pun, Appl. Surf. Sci. **357**, 1097 (2015).
[12] R. H. Kim, H. H. Park, G. T. Joo, Appl. Surf. Sci. **169-170**, 564 (2001).
[13] E. M. Standifer, D. H. Jundt, R. G. Norwood, P. F. Bordui, Proceedings of the Annual IEEE International Frequency Control Symposium. Pasadena, USA, 470 (1998).
[14] Y. Long, M. Yu, H. Li, Z. Shi, L. Wang, Y. Ding, Y. Xu, Z. Wu, Piezoelectrics & Acoustooptics **41**, 340 (2019).
[15] X. F. Xiao, H. Zhang, X. F. Zhang, J. Mater. Sci. Mater. Electron. **31**, 16414 (2020).

*Corresponding author: xxf666666@163.com